Origin of correlated isolated flat bands in copper-substituted lead phosphate apatite.

Sinéad M. Griffin[1,2]
[1]*Materials Sciences Division, Lawrence Berkeley National Laboratory, Berkeley, California, 94720, USA and*
[2]*Molecular Foundry Division, Lawrence Berkeley National Laboratory, Berkeley, California, 94720, USA*
(Dated: August 1, 2023)

A recent report of room temperature superconductivity at ambient pressure in Cu-substituted apatite ('LK99') has invigorated interest in the understanding of what materials and mechanisms can allow for high-temperature superconductivity. Here I perform density functional theory calculations on Cu-substituted lead phosphate apatite, identifying correlated isolated flat bands at the Fermi level, a common signature of high transition temperatures in already established families of superconductors. I elucidate the origins of these isolated bands as arising from a structural distortion induced by the Cu ions and a chiral charge density wave from the Pb lone pairs. These results suggest that a minimal two-band model can encompass much of the low-energy physics in this system. Finally, I discuss the implications of my results on possible superconductivity in Cu-doped apatite.

INTRODUCTION

High-T_C superconductors are arguably the holy grail of condensed matter physics with huge potential applications for an energy-efficient future. The first class of superconductors that were considered to be high-T_C were the cuprates which were discovered by Bednorz and Müller in 1987 [1]. The cuprates have been subsequently followed by several new classes including the Fe-pnictides in 2008 [2] and the nickelates [3].

While significant strides have been made in the discovery and understanding of high-T_C superconductors, and we continue to unearth novel examples within established classes [4], a definitive roadmap to achieving room-temperature T_C under ambient pressures has remained elusive. Common to many of these high-T_C superconducting families are strongly correlated bands which can give rise to unconventional mechanisms for Cooper pair formation [5, 6], and proximity to multiple competing interactions such as antiferromagnetism, charge density waves and spin-density waves. These phases can compete or coexist with superconductivity where fluctuations between these states are believed to play a significant role for achieving high-T_C. Searching for these features in new materials systems is therefore a promising route for finding new classes of high-T_C superconductors. For instance, the nickelate supercondcutors were originally predicted in theory by Anisimov, Bukhvalov and Rice as an analogy to the cuprate superconductors [7]. Similar approaches have also been proposed to selectively design a material with the sought-after isolated d-manifold that is associated strong correlations [8], and have inspired high-throughput searches for good candidate materials, further expanding the horizons of high-Tc superconductivity [9].

The recent report of possible room temperature superconductivity at ambient pressures in Cu-substituted apatite (also known as 'LK99')[10, 11] motivates the need for a thorough understanding of the structure-property relationships in these compounds to begin to unravel their potential correlated physics. In this Letter, I use *ab initio* calculations to elucidate the key completing interactions in Cu-doped apatite at the mean-field density functional level.

METHODS

I used the Vienna Ab initio Simulation Package (VASP) [12–15] for all density functional theory (DFT) calculations with full calculation details given in the SI. I applied a Hubbard-U correction to account for the underlocalization of the Cu-*d* states. I tested values of U between 2 eV and 6 eV, finding my results were similar for all values calculated. The results in the main text are for U = 4 eV which gives lattice parameters within 1% of experiment [10, 16].

RESULTS

Structural Properties

Apatites are materials with the general formula $A_{10}(TO_4)_6X_{2\pm x}$, where A = alkaline or rare earth metal; M = Ge, Si, or P; and X = halide, O, or OH. The name 'apatite' derives from the Greek *apatē* meaning 'deceit' as a result of the diverse range of forms it can take [17]. Here I consider the lead-phosphate apatite $Pb_{10}(PO_4)_6(OH)_2$. Taking its structure reported from X-ray diffraction in Ref. [16] as the starting point, its relaxed following a structural optimization is depicted in Fig. 1. It adopts the typical crystal structure of various apatite chemistries, namely it forms a network comprising PbO_6 prisms that are corner shared with PO_4 tetrahedra. I refer to these Pb as Pb(1), in keeping with the convention in literature [18]. This framework is filled with $Pb_6(OH)_2$ where the $(OH)_2$ forms a chain in the

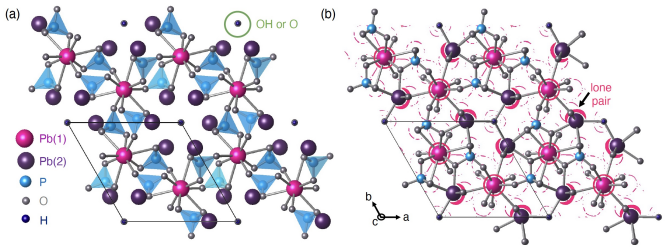

FIG. 1. (a) Lead-phosphate apatite structure with two inequivalent Pb sites as described in the main text. Columns of O or OH sit in the center column defined by Pb(2) hexagonal structure. (b) Calculated electronic localization function for $Pb_{10}(PO_4)_6OH_2$. Oxygens surrounding Pb(2) are repelled by the lone pair.

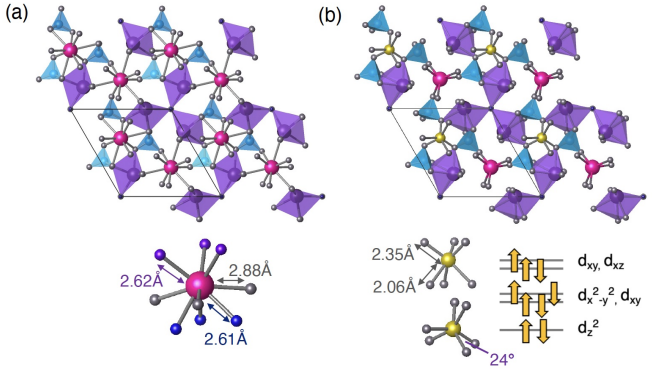

FIG. 2. (a) Lead-phosphate apatite structure showing nine-coordinated Pb(1) sites. (b) Cu-substituted structure showing six-coordinated Cu and Pb(1) sites with distorted trigonal prism coordination with two different bondlengths are a rigid twist of $\sim 24^\circ$ between the upper and lower triangles. A cartoon of the resulting crystal-field diagram for Cu-d^9 is given on the right.

center of a hexagonal structure defined by these Pb(2) atoms. While here I consider OH^{-1} filling the hexagonal column, I obtained similar results for O only in the column. Typically apatites adopt the hexagonal $P6_3/m$ space group – here our resulting structure has $P6_3$ owing to the breaking of reflection from the OH molecule ordering. However, small structural deviations from the $P6_3/m$ commonly occur depending on its constituents.

While the Pb(1) forms the overall framework with the PO_4 tetrahedra, the Pb(2) play a crucial role in Pb-O connectivity and polyhedra tilts throughout the structure. In fact, while both Pb(1) and Pb(2) possess $6s^2$ lone pairs, only the latter is stereochemically active. I verify this by calculating the electronic localization function (ELF) as shown in Fig. 1(b), finding that the Pb(2) lone pairs form a chiral arrangement that make angle of $\sim 105^\circ$ with the a-axis (see SI for more details). The chiral arrangement of the lone pairs sets the resulting oxygen coordination of the Pb(2), namely its six oxygens are arranged asymmetrically as a result of their repulsion from the lone pair forming a chiral charge density wave. Since these oxygen are corner shared with the PO_4, the structural distortions associated with the Pb(2) lone pair activity propagate throughout the structure. Such an effect has been discussed previously in various apatite materials, noting that the lone pair ordering differs depending on the specific system [18, 19].

I next consider the substitution of Cu on a Pb(1) site resulting in $CuPb_9(PO_4)_6OH_2$, with the fully optimized structure shown in Fig. 2(b). I find several changes to the structure with the inclusion of Cu. Firstly, all lattice parameters decrease with a going from 9.875 Å to 9.738 Å and c going from 7.386 Å to 7.307 Å. While my calculated lattice parameters agree well with those reported in Ref.[10], I find a greater structure collapse than their report of a going from 9.865 Å without Cu to 9.843 Å with Cu, and c going from 7.431 Å without Cu to 7.428 Å with Cu. Interestingly, I find Cu substitution results in a global structural distortion that results in a change in coordination from nine to six (with a cutoff of 3 Å) not only for the Cu on the Pb(1) site, but also for all other Pb(1) sites. This results in a modification of the polyhedral tilts throughout the structure, most notably in the PO_4 polyhedra, as seen in Fig. 2(b). I classify the distortion through analysis of the symmetry-adapted phonon modes before and after Cu substitution finding the structural distortion to be caused by Γ_1 and Γ_2 modes of amplitudes 1.19Å and 1.78Å respectively. Visualization of these symmetry-adapted modes is given in the SI (Fig. S1); this analysis confirms that the structural distortion caused by the Cu substitution on Pb(1) is primarily driven by polyhedral tilts of the PO_4 and their corner-shared oxygen neighbors.

Looking closely at the change in coordination of Cu on the Pb(1) site, I see the Cu^{2+} is now six-coordinated with oxygen forming a distorted Jahn-Teller trigonal prism. In an ideal trigonal prism the anions are arranged at the vertices of a regular triangular prism with the transition metal at the center with D_{3h} symmetry. However, breaking in-plane mirror symmetry results in Jahn-Teller distorted trigonal crystal field with C_{3v} symmetry, such as is found in the Janus compounds [20]. Here I find the mirror is already broken by the next-nearest neighbor P ions the Cu-O distance that has nearby P is 2.06 Å, whereas the Cu-O without surround P ions is 2.35 Å. Such out-of-plane asymmetry in the Cu environment results in a local dipole in z which can also influence the resulting electronic structure [20]. In addition to the mirror symmetry breaking, the O triangles are also rotated at a small angle of $\sim 24^\circ$ with respect to each other, referred to as a Bailar twist in molecules[21], giving the final distorted trigonal prism. Interestingly, the same structural distortion has been observed upon substitution of U on the Ca(1) site in fluorapatite $Ca_{10}(PO_4)_6F_2$ as measured from X-ray absorption spectroscopy [22]. There the authors found that

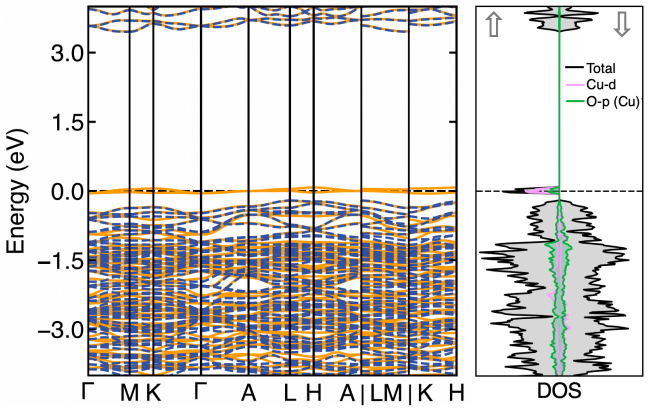

FIG. 3. Calculated spin-polarized electronic band structure (left) and corresponding density of states (right). The spin-up bands are depicted in solid orange, and the spin-down bands are dashed blue. The total density of states is shaded grey with projections shown of the Cu-d orbitals (pink) and its neighboring O-p orbitals (green). In both plots the Fermi level is set to 0 eV and is marked by the dashed line.

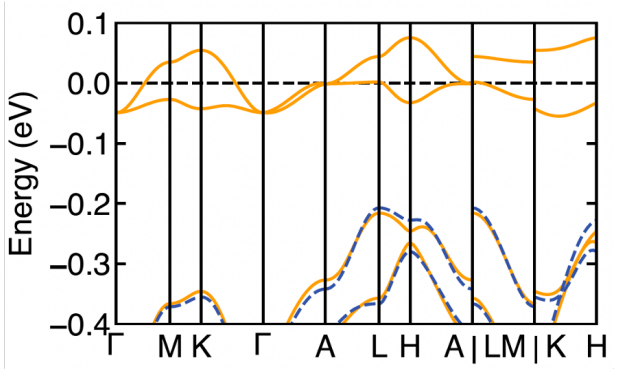

FIG. 4. Calculated spin-polarized electronic band structure in smaller energy range around the Fermi level showing the isolated two-band Cu-d manifold. The Fermi level is set to 0 eV and is marked by the dashed line.

the U substitution on the Ca(1) sites causes an usual 6-coordinated structure – a trigonal prism with six equal bondlengths of 2.06Å with an undetermined Bailar twist angle, however.

Electronic Structure

I present the calculated spin-polarized electronic structure in Fig. 3. Remarkably, I find an isolated set of flat bands crossing the Fermi level, with a maximum bandwidth of ∼130 meV (see Fig.4) that is separated from the rest of the valence manifold by 160 meV. Such a narrow bandwidth is particularly indicative of strongly correlated bands. These especially flat bands are consistent with the Cu-O coordination where I find Cu-O bondlengths of 2.35 Å and 2.06 Å in the distorted trigonal prism. For comparison, the Cu-O bondlengths in the cuprate superconductors are typically $\leq$ 2Å (in-plane) and $\leq$ 2.3Å (apical) [3], giving further evidence of the unusual coordination and resulting band localization in this isolated Cu-d manifold.

The crystal-field splitting for the trigonal prism comprises a single d_{z^2}, doubly degenerate d_{xy} and $d_{x^2-y^2}$, and doubly degenerate d_{yz} and d_{xz}. In fact, the relative positioning of the d_{z^2} and the d_{yz}/d_{xz} is set by the anisotropy induced by the mirror-symmetry breaking large values of asymmetry can cause the d_{z^2} to be destabilized. In our case for Cu^{2+} with a d^9 configuration I expect half filling of the doubly degenerate d_{yz}/d_{xz} bands - this is corroborated with our calculations in Fig. 3 where I find two bands of d_{yz}/d_{xz} character at Fermi level that are are half filled. My results suggest that low-energy physics of this system can be described by a two-band d_{yz}/d_{xz} model, similar to that originally suggested for Fe-pnictide superconductors [23, 24]. However, unlike other correlated-d band superconductors, in this system the Cu-d bands are particularly flat – there is minimal band broadening from neighboring oxygen ions. If previous assumptions about band flatness driving superconductivity are correct, then this result would suggest a much more robust (higher temperature) superconducting phase exists in this system, even compared to well-established high-T_C systems.

While the calculations presented here are performed for GGA+U with a U = 4 eV applied to the Cu-d, I find the same qualitative features of the band structures for a wide range of U values, as presented in the SI. This suggests that the presence of such an isolated manifold of flat Cu-d bands is a feature of the structural reconstruction and new crystal field environment provided by the apatite network. I further confirm this by calculating the band structure of the Cu-substituted compound without performing a structural relaxation, that is, taking structure of the ideal $Pb_{10}(PO_4)_6(OH)_2$ and replacing a Pb(1) with Cu without allowing the structure to relax. In this case, I find slight spin-polarization in the band structure, however all Cu-d states are now in the bulk valence manifold and do not form an isolated manifold (see SI Fig. S3). Finally, the top of the valence band is made up of the Pb(2)-s states, confirming their contribution to the stereochemical activity of the lone pairs (see SI).

I next investigate the exchange interactions between Cu ions in different unit cells by constructing doubled unit cells in the in-plane and out-of-plane directions. I find that there is a preference of 2 meV/Cu for ferromagnetic coupling in the out-of-plane direction (with a Cu-Cu separation of $c = 7.307$ Å), whereas a preference of 7 μeV/Cu for antiferromagnetic coupling in the in-plane direction (with a Cu-Cu separation of $a = 9.738$Å). However, while this result is indicative of the potential exchange interactions in the system, it relies on the unrealistic assumption that the Cu ions will sit on the same

substitution position in each unit cell. A full study of potential exchange interactions for various Cu locations is out of the scope of this work, and will crucially be informed by the Cu locations determined in experiment.

So far all calculations have been for Cu on the Pb(1) site, which is the site occupancy reported in Ref.[10]. I also calculated the structural and electronic properties of Cu in the Pb(2) site with the resulting structure and bands given in the SI. In this location, the Cu interrupts the hexagonal network that is characteristic of the apatite structure, which causes a structural rearrangement to the lower $P1$ symmetry. The Cu substituted in this position is now tetrahedrally coordinated by oxygen, and has a significantly different electronic structure with no correlated d bands crossing the Fermi level, as detailed in the SI. In fact, I find that Cu on this Pb(2) is 1.08 eV more energetically favorable that Cu on the Pb(1) site, suggesting possible difficulties in robustly obtaining Cu substituted on the Pb(1) site.

DISCUSSION

These theoretical results suggest that the apatite structure provides a unique framework for stabilizing highly localized Cu-d^9 states that form a strongly correlated flat band at the Fermi level. The central role of stereochemically active $6s^2$ lone pairs of Pb(2) manifests in the formation of a chiral charge density wave and the propagation of structural distortions with connected polyhedra. When Cu is substituted on a Pb(1) site, the result is a cascade of structural alterations, including reduced lattice parameters, changes in coordination, and modified polyhedral tilts, leading to a local Jahn-Teller distorted trigonal prism around Cu. This results in an unusually flat set of isolated d_{yz}/d_{xz} bands with half-filling.

I briefly note that achieving such a crystal field environment should also be possible in intercalated twisted heterogeneous bilayers where selection of different heterobilayers can provide the mirror symmetry breaking, while moiré twist can provide an arbitrary rotation of the upper and lower triangles. In fact such a platform would be ideal for probing the physics found here given its broad range of tunability and the state-of-the-art characterization probes for their interrogation [25].

I now discuss the potential implications of these features of Cu-substituted apatite for possible high-T_C superconductivity, and in particular the role of the flat bands and the presence of competing magnetic interactions and phonons. Isolated, flat bands have long been a target for achieving high-T_C as predicted from BCS theory[26–28]. The critical temperature T_C given by by $T_C \propto \exp(-1/|U|\rho_0(E_F))$, where $|U|$ is the magnitude of the effective attractive interaction and $\rho_0(E_F)$ is the density of states at the Fermi surface. In a flat band where the density of states diverges, T_C is proportional to $|U|$. This suggests that, at low interaction strengths, the critical temperature in flat bands could be significantly enhanced, as is currently being explored in various moiré systems[29]. In our case, the correlated bands have a bandwidth of ~ 130 meV which is less than their separation from the rest of the valence manifold (160 meV) at the level of density functional theory. While strong correlations will need to be taken into account adequately to accurately describe these scenarios, these are promising hints for these proposals that predicts that the T_C is proportional to the interaction strength.

In contrast to conventional superconductors, where phonon-mediated interactions govern Cooper pair formation, there is wide consensus that other bosonic excitations are responsible for the attractive pair formation in high-T_C superconductors ranging from paramagnons to spin- and charge-density waves [30]. In this system, I have identified several potential sources of fluctuations that could contribute to pairing. Firstly, I identified a charge density wave (CDW) driven by chiral lone pair ordering on the Pb(2) sites – the presence of this CDW is strongly connected to the structural rearragement that occurs when Cu is incorporated into the Pb(1) lattice sites. In addition to this, I identified two zone-center phonon modes that trigger the global structural deformation that occurs as a result of the Cu substitution, suggesting potentially strong electron-phonon coupling for these modes. Finally, I calculated the relative exchange interactions between Cu in neighboring unit cells. Interestingly for the out-of-plane coupling, that is, along the Cu-Pb-Cu one-dimensional chains, I find ferromagnetic coupling is favored by 2 meV/Cu over antiferromagnet coupling, even though the Cu are over 7 Å apart, suggesting that spin fluctuations could also play a key role.

Finally, the calculations presented here suggest that Cu substitution on the appropriate (Pb(1)) site displays many key characteristics for high-T_C superconductivity, namely a particularly flat isolated d-manifold, and the potential presence of fluctuating magnetism, charge and phonons. However, substitution on the other Pb(2) does not appear to have such sought-after properties, despite being the lower-energy substitution site. This result hints to the synthesis challenge in obtaining Cu substituted on the appropriate site for obtaining a bulk superconducting sample. Nevertheless, I expect the identification of this new material class to spur on further investigations of doped apatite minerals given these tantalizing theoretical signatures and experimental reports of possible high-T_C superconductivity.

Acknowledgements-. I am grateful to David Prendergast, Adam Schwartzberg, Shuhada' Sadaqat and John Vinson for insightful discussions and encouragement. I also thank D. Kwabena Bediako, Donnie Evans, Adam Schwartzberg and John Vinson for feedback on this draft. This work was funded by the U.S. Department of Energy, Ofce of Science, Ofce of Basic Energy Sciences,

Materials Sciences and Engineering Division under Contract No. DE-AC02-05-CH11231 within the Theory of Materials program. Computational resources were provided by the National Energy Research Scientific Computing Center and the Molecular Foundry, DOE Office of Science User Facilities supported by the Office of Science, U.S. Department of Energy under Contract No. DEAC02-05CH11231. The work performed at the Molecular Foundry was supported by the Office of Science, Office of Basic Energy Sciences, of the U.S. Department of Energy under the same contract.

[1] J. G. Bednorz and K. A. Müller, Zeitschrift für Physik B Condensed Matter **64**, 189 (1986).
[2] Y. Kamihara, T. Watanabe, M. Hirano, and H. Hosono, Journal of the American Chemical Society **130**, 3296 (2008).
[3] D. Li, K. Lee, B. Y. Wang, M. Osada, S. Crossley, H. R. Lee, Y. Cui, Y. Hikita, and H. Y. Hwang, Nature **572**, 624 (2019).
[4] G. A. Pan, D. Ferenc Segedin, H. LaBollita, Q. Song, E. M. Nica, B. H. Goodge, A. T. Pierce, S. Doyle, S. Novakov, D. Córdova Carrizales, et al., Nature materials **21**, 160 (2022).
[5] V. Khodel and V. Shaginyan, Jetp Lett **51**, 553 (1990).
[6] T. T. Heikkilä and G. E. Volovik, Basic Physics of Functionalized Graphite pp. 123–143 (2016).
[7] V. Anisimov, D. Bukhvalov, and T. Rice, Physical Review B **59**, 7901 (1999).
[8] S. M. Griffin, P. Staar, T. C. Schulthess, M. Troyer, and N. Spaldin, Physical Review B **93**, 075115 (2016).
[9] E. B. Isaacs and C. Wolverton, Physical Review X **9**, 021042 (2019).
[10] S. Lee, J.-H. Kim, and Y.-W. Kwon, arXiv preprint arXiv:2307.12008 (2023).
[11] S. Lee, J. Kim, H.-T. Kim, S. Im, S. An, and K. H. Auh, arXiv preprint arXiv:2307.12037 (2023).
[12] G. Kresse and J. Hafner, Phys. Rev. B **47**, 558 (1993), ISSN 01631829.
[13] G. Kresse and J. Hafner, Phys. Rev. B **49**, 14251 (1994), ISSN 0163-1829, URL `http://link.aps.org/doi/10.1103/PhysRevB.49.14251`.
[14] G. Kresse and J. Furthmüller, Comp. Mater. Sci. **6**, 15 (1996), ISSN 09270256.
[15] G. Kresse and J. Furthmüller, Phys. Rev. B **54**, 11169 (1996), ISSN 0163-1829, URL `http://link.aps.org/doi/10.1103/PhysRevB.54.11169`.
[16] S. Brückner, G. Lusvardi, L. Menabue, and M. Saladini, Inorganica Chimica Acta **236**, 209 (1995).
[17] P. D. Roycroft and M. Cuypers, Irish Journal of Earth Sciences **33**, 71 (2015).
[18] J. Peet, A. Piovano, M. Johnson, and I. R. Evans, Dalton Transactions **46**, 15996 (2017).
[19] S. M. Antao and I. Dhaliwal, Journal of Synchrotron Radiation **25**, 214 (2018).
[20] D. Er, H. Ye, N. C. Frey, H. Kumar, J. Lou, and V. B. Shenoy, Nano letters **18**, 3943 (2018).
[21] J. C. Bailar Jr, Prep. Inorg. React **1**, 1 (1964).
[22] J. Rakovan, R. J. Reeder, E. J. Elzinga, D. J. Cherniak, C. D. Tait, and D. E. Morris, Environmental Science & Technology **36**, 3114 (2002).
[23] Q. Han, Y. Chen, and Z. Wang, Europhysics Letters **82**, 37007 (2008).
[24] S. Raghu, X.-L. Qi, C.-X. Liu, D. J. Scalapino, and S.-C. Zhang, Phys. Rev. B **77**, 220503 (2008), URL `https://link.aps.org/doi/10.1103/PhysRevB.77.220503`.
[25] M. Van Winkle, I. M. Craig, S. Carr, M. Dandu, K. C. Bustillo, J. Ciston, C. Ophus, T. Taniguchi, K. Watanabe, A. Raja, et al., Nature Communications **14**, 2989 (2023).
[26] T. T. Heikkilä, N. B. Kopnin, and G. E. Volovik, JETP letters **94**, 233 (2011).
[27] N. Kopnin, T. Heikkilä, and G. Volovik, Physical Review B **83**, 220503 (2011).
[28] J. S. Hofmann, E. Berg, and D. Chowdhury, Physical Review B **102**, 201112 (2020).
[29] P. Törmä, S. Peotta, and B. A. Bernevig, Nature Reviews Physics **4**, 528 (2022).
[30] E. Bertel and A. Menzel, Symmetry **8**, 45 (2016).